Supporting Information

Sustainable production of glucaric acid from corn stover via glucose oxidation: an assessment of homogeneous and heterogeneous catalytic oxidation production routes

Vaishali Thaore[*1], Robert D. Armstrong*[2], Graham J. Hutchings*[2], David W. Knight*[2], David Chadwick*[1], Nilay Shah*[1]

S.I ASPEN Process model details for Corn stover conversion to glucaric acid

This section provides additional details of the process model. A schematic process flow diagram is shown in Figure S.1. The composition of the corn stover feedstock is given in Table S.1. The glucaric acid production process model was designed in ASPEN Plus V9. The physical and chemical properties of all components (except glucaric and potassium glucarate) were assigned according to the Aspen Plus V9 database and property data developed by the National Renewable Energy Laboratory (NREL) for biochemical conversion of lignocellulosic biomass to ethanol (Humbird et al., 2011). The physicochemical properties of glucaric acid and potassium glucarate components were estimated based upon their molecular structures as given in Table S.2. the reactions for process areas concerned with acid pre-treatment (A200), ammonia conditioning and acidification (A200), and cellulose conversion to glucose (A300) are given in Table S.3. An overall process flow diagram for Route 1 is given in Figure S.2.

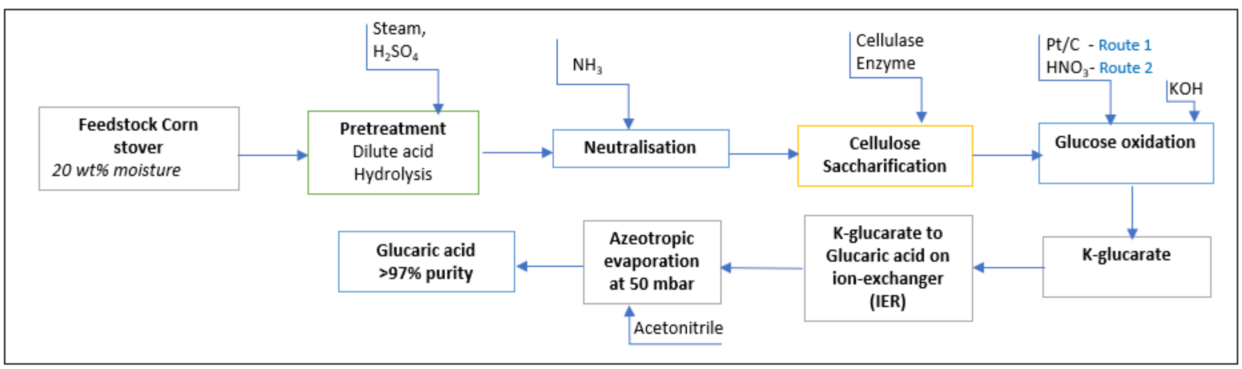

Figure S.1: Process flow diagram for Glucaric acid production from corn stover

Table S.1: The composition of corn stover biomass

Component	Mass fraction (dry basis)
Cellulose	0.3895
Xylan	0.2831
Lignin	0.1346
Acetate	0.0635
Ash	0.0489
Arabinan	0.0476
Galactan	0.0159
Protein	0.01
Mannan	0.0069

Table S.2: Physio-chemical property data for ASPEN model

Property	Value	Units	Reference
Glucaric acid			
OMEGA	1.6788		Specify molecular structure, Aspen property estimation tool using-NIST TDE
ZC	0.193		
VC	0.4605	cum/kmol	
PC	2.93E+06	N/sqm	
TC	841	K	
MW	210.14		
TB	675.5	K	
SG	1.897		
VLSTD	0.1109	cum/kmol	
ΔH_{fg}	-1510	kJ/mol	Vasiliu et al., 2011
ΔH_{vap}	138	kJ/mol	
ΔH_{liq}	-1648	kJ/mol	
Potassium glucarate solid			
MW	248.23		Modelled as solid component, properties were estimated by specifying molecular structure.
Melting point	461	K	
PLXANT/1	$-1e^{20}$	Atm	Forced as non-volatile component.
Heat of fusion	46793	J/mol	The solubility of K-glucarate in water as 0.07 M which corresponds to 17.37 g/l (Armstrong et al., 2017; Joback and Reid, 1987)

Table S.3: Reactions in process area A200–A300

Reaction No.	Reaction	Temperature (K)	Pressure (MPa)	% Conversion
Reactions in Process area A200 -Dilute acid pre-treatment				
R1	$Cellulose + H_2O \xrightarrow{H_2SO_4} Glucose$	373, 431	0.7, 0.57	$X_{Cellulose} = 0.099$
R2	$Cellulose \xrightarrow{H_2SO_4} HMF + 2H_2O$	373, 431	0.7, 0.57	$X_{Cellulose} = 0.003$
R3	$Xylan + H_2O \xrightarrow{H_2SO_4} Xylose$	373, 431	0.7, 0.57	$X_{Xylan} = 0.9$
R4	$Xylan \xrightarrow{H_2SO_4} Furfural + 2H_2O$	373, 431	0.7, 0.57	$X_{Xylan} = 0.05$
R5	$Arabinan + H_2O \xrightarrow{H_2SO_4} Arbinose$	373, 431	0.7,0.57	$X_{Arabinan} = 0.9$
R6	$Galactan + H_2O \xrightarrow{H_2SO_4} Galactose$	373, 431	0.7, 0.57	$X_{Galactan} = 0.9$
R7	$Acetate \xrightarrow{H_2SO_4} C_2H_4O_2$	373, 431	0.7, 0.57	$X_{Acetate} = 1$
R8	$HMF + 3H_2O \xrightarrow{H_2SO_4} TAR$	373, 431	0.7, 0.57	$X_{HMF} = 1$
R9	$Furfural + 3H_2O \xrightarrow{H_2SO_4} TAR$	373, 431	0.7, 0.57	$X_{Furfural} = 1$
Ammonia conditioning and Re-acidification				
R10	$C_2H_4O_2 + NH_3 \longrightarrow NH_4^+C_2H_3OO^{2-}$	350	0.57	$X_{C_2H_4O_2} = 1$
R11	$H_2SO_4 + 2NH_3 \longrightarrow (NH_4^+)_2SO_4^{2-}$	350	0.57	$X_{H_2SO_4} = 1$
R12	$Xylose \longrightarrow TAR$	350	0.57	$X_{Xylose} = 0.01$
R13	$H_2SO_4 + 2NH_3 \longrightarrow (NH_4^+)_2SO_4^{2-}$	350	0.34	$X_{H_2SO_4} = 1$
Reactions in Process area A300				
R14	$Cellulose + H_2O \xrightarrow{Cellulase} Glucose$	321	0.1	$X_{Cellulose} = 0.9$

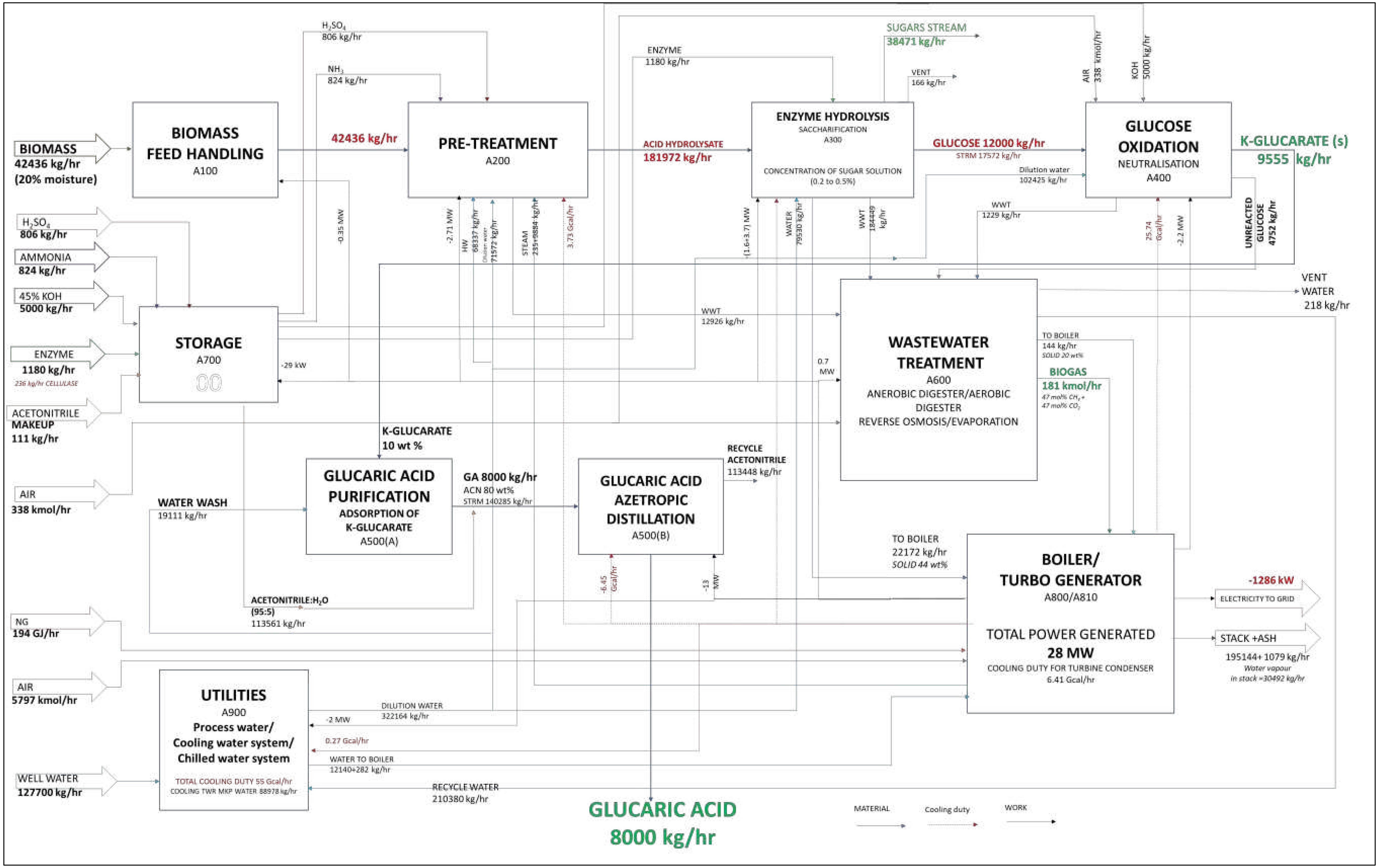

Figure S.2: The overall process flow diagram for Route 1-Glucaric acid production from corn stover biomass

S.II Pore Diffusion model Equations

Simulation of the fixed bed adsorption column including pore diffusion model kinetics and Langmuir adsorption model was performed in the gPROMS process modelling platform for an adsorption column of 4 m length and 1 m diameter. The adsorption parameters are given in Table S.4. A detailed simulation of the GA concentration profile with respect to bed height is shown in Figure S.3. Based on the simulation results for the purification process, 8 ion exchange columns (4 for adsorption and 4 in regeneration) were required to adsorb 9555 kg/hr of K-glucarate in Route 1 each having a length of 4m and a diameter of 1m. Whereas in Route 2, 6 columns of the same dimensions were required (3 for adsorption and 3 in regeneration) for adsorption of 7279 kg/hr of K-glucarate. A total of 26875 kg of ion exchange resin (IER) was loaded into columns for Route 1 and 20625 kg for Route 2.

The mass balance equations used for bed (Eq S.1) and particle (Eq. S.2) are as follows

$$\frac{\partial c_{GA}}{\partial t} = D_L \frac{\partial^2 c_{GA}}{\partial L^2} - u \frac{\partial c_{GA}}{\partial L} - \left(\frac{3(1-\varepsilon)}{\varepsilon r_p} \varepsilon_p D_p \left. \frac{\partial c_p}{\partial r} \right|_{r=r_p} \right) \quad \text{(Eq. S.1)}$$

$$\varepsilon_p \frac{\partial c_p}{\partial t} + \left(1-\varepsilon_p\right) \frac{\partial q}{\partial t} = \frac{\varepsilon_p}{r^2} \frac{\partial}{\partial r} \left[r^2 D_p \frac{\partial c_p}{\partial r} \right]_L \quad \text{(Eq. S.2)}$$

$$q = \frac{q_m c_p}{K_d + c_p} \quad \text{(Eq. S.3)}$$

Boundary condition for bed and particle are

at z=0

$$D_L \frac{\partial c_{GA}(0,t)}{\partial z} = u(c_{GA}(0,t) - c_{GA_0})$$

at z=L

$$\frac{\partial c_{GA}}{\partial z}(L,t) = 0$$

Boundary condition for particle are

at r=0

$$\frac{\partial c_p}{\partial r}(o,z,t) = 0$$

at r=r_p

$$c_p(r_p, z, t) = c_{GA}(z)$$

Initial conditions for bed and particle are

at t=0

$$c_{GA}(z, 0) = 0$$

at z=0

$$c_{GA}(0, t) = c_0$$

Initial condition for particle

$$c_p(r, z, 0) = 0$$

Table S.4: Adsorption parameters

Resin (Yuan *et al.*, 2017)	Density ($gm.ml^{-1}$)	Particle Radius (mm)	Langmuir Parameter		D_L ($m^2.s^{-1}$) Dispersion coefficient in column	D_P ($m^2.s^{-1}$) Pore diffusion coefficient
			q_m ($mg.ml^{-1}$)	K_D ($mg.ml^{-1}$)		
Ion-exchange resin Polystyrene	1.25	1.25	113.94	0.04	11.3×10^{-10}	11.3×10^{-11}

For, column diameter = 1m and column length = 4m,

For 10 wt % K-Glucarate solution,

$c_{GA_0} = 100\ kg.m^{-3}$

U=Vol flow rate/Cross Sectional area of column (m/sec)

c_{GA} concentration of glucaric acid in external liquid [kg. m^{-3}];

c_p intra-particle concentration of glucaric acid [kg. m^{-3}];

D_L Dispersion coefficient in column [$m^2.sec^{-1}$];

D_p Glucaric acid diffusivity in IER particle [$m^2.sec^{-1}$];

K_D Langmuir adsorption parameter [$kg.m^{-3}$];

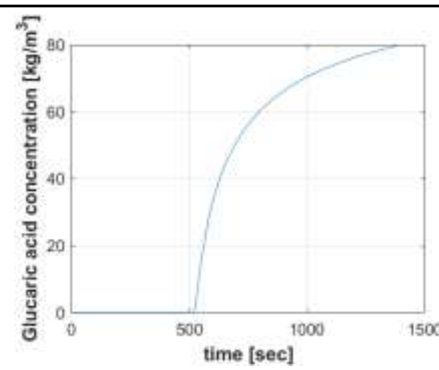

Figure S.3: Concentration profile for glucaric acid in the adsorption column with 4m length and 1m column diameter

L length of column [m]; q amount of glucaric acid adsorbed on IER at equilibrium [$kg.m^{-3}$]; q_m maximum capacity of resin [$kg.m^{-3}$]; R radius of particle [m]; r_p radial distance in particle [m]; t time [sec]; u superficial velocity [$m.sec^{-1}$]; z linear distance in column [m]; ε bed voidage, ε_p bed porosity

Fixed bed adsorption column for cation-ion exchange resin Amberlyst-15

The resin column parameters were also evaluated based on the Amberlyst-15 resin capacity provided by the resin manufacturer.

Amberlyst-15 (AMBERLYST^{TM} 15WET)

Resin density- 770 g/l and

Ion-exchange capacity, 1.7 eq/l

$$\text{Minimum potassium ion loading} = \frac{1.7\times 39}{770}\left(\frac{\text{g}}{\text{kg of resin}}\right)$$

$$= 86\left(\frac{\text{g}}{\text{kg of resin}}\right)$$

Adsorption capacity, q_{max} = 116.5 g/kg resin (Miller et al., 2015)

Assumptions: Adsorption capacity = 100 g/kg resin,

For Column dimensions: length = 4m, diameter = 1m

Column volume=(πd^2)/4 L= 3.14 m^3

Feed flow rate for one column = 24387.5 kg/hr (10 wt% potassium glucarate)

$$\text{K}^{+}\text{adsorbed (kg)} = \text{Column volume (m}^3) \times \text{resin density(kg/m}^3) \times \text{adsorption capacity (kg of adsorbate/kg adsorbent)}$$

$$\text{Potassium ion adsorbed} = 3.14 \times 770 \times 0.1 = 241.78\ \text{kg}$$

$$\text{Potassium ion loading} = \frac{1.7\times 39}{770}\ \text{g/kg of resin} = 86\ \text{g/kg of resin}$$

$$\text{Adsorption cycle time (h)} = \frac{\text{Potassium ion adsorbed (kg)}}{\text{Potassium ion loaded in feed(kg/h)}} = \frac{241.78}{24387.5\times 0.1 * 0.15} = 0.66\ \text{h} = 40\ \text{min}$$

SIII. Data for financial and environmental analysis

This section provides data for financial and environmental analysis. The unitary cost data for input streams is given in Table S.5. The discounted cash flow analysis method was used to determine a minimum selling price for GA by equating the net present value to zero at the end of 20 years (Peters et al., 2003). Table S.6 summarises the discounted cash flow analysis parameters for the new glucaric acid production plant assuming 35% income tax rate, 40% project contingency, 6 years of capital depreciation (200 % declining balance - DB method of depreciation), and minimum acceptable annual rate of return (MARR) of 15%. The CO_2 emission factor for each input stream is given in Table S.7. Based on CO_2 emission factor and consumption of raw materials, the total GHG emissions for glucaric acid production process via Route 1 and Route 2 was estimated. The values are given in Table S.8.

Table S.5: Unitary cost of input streams

Components **With cost source**	**USD /tonne or** **USD/Unit**
Corn stover biomass (Humbird et al., 2011)	88.20
(ICIS, 2017) H_2SO_4	73.87
(ICIS, 2017) NH_3	638.37
(JBEI, 2009) Cellulase	3274.76
(ICIS, 2017) HNO_3 (67%)	286.66
(ICIS, 2017) KOH (45%)	364.23
(ICIS, 2017) Acetonitrile	1578
(Humbird et al., 2011) Water	0.28
(EIA; Humbird et al., 2011) Electricity (kWhr)	0.065
(EIA) NG (GJ)	7.41
(SIGMA ALDRICH, 2018) Pt catalyst	5240
(AMBERLYST, 2018) IER cost	1267

Table S.6: Parameters for Discounted cash flow analysis

Parameters	**Assumption**
Plant life	20 yrs
Plant operational annual hours	8400 hrs
Construction time	36 months
Capital depreciation	6 years 200 % declining balance (DB) method of depreciation
Minimum acceptable annual rate of return (MARR)	15 %
Income tax rate	35 %
Equity financing	100%

Table S.7: CO_2 emission factors for input streams in glucaric acid production process models

Input	**Emission factor (kg of CO_2eq/tonne)**	**Sources for CO_2 Emission factor**
Biomass	59.44	(Giarola et al., 2012)
H_2SO_4	135.85	(Frischknecht et al., 2005)
NH_3	2311.14	(Frischknecht et al., 2005)
Enzymes	7717.75	(Slade et al., 2009)
HNO_3 (50% in H_2O)	3017*	(US EPA, 2009; Jungbluth et al., 2007)
KOH (45 % in H_2O)	2906*	(Jungbluth et al., 2007)
Acetonitrile	180	(Frischknecht et al., 2005)
Water	0.74	(Frischknecht et al., 2005)
NG (energy)	1.99	(Giarola et al., 2016)

**from eco-invent (database 3.4, allocation at the point of substitution and IPCC 2013),*

GWP_{20} = 3.0177 kg CO_2eq/kg HNO_3, GWP_{20} = 2.9069 kg CO_2eq/kg KOH

Table S.8: Total GHG emissions for glucaric acid production process via Route 1 and Route 2

Input streams	**Route 1**	**Route 2**
Acetonitrile	2.55	2.56
Water	11.55	14.60
Sulphuric acid	13.70	18.01
Natural gas	48.25	63.47
Nitric acid	0.00	217.46
Cellulase	228.32	300.13
Ammonia	237.90	312.72
Corn stover biomass	315.26	414.41
Potassium hydroxide	818.38	806.84
Total GHG emissions in kg CO2 eq/tonne of Glucaric acid	**1675**	**2150**

References

AMBERLYST^{TM} 15WET Industrial Grade Strongly Acidic Catalyst. URL www.lenntech.com. (accessed 3.12.18)

Armstrong, R.D., Kariuki, B.M., Knight, D.W., Hutchings, G.J., 2017. How to Synthesise High Purity, Crystalline d-Glucaric Acid Selectively. European J. Org. Chem. 2017, 6811–6814. https://doi.org/10.1002/ejoc.201701343

EIA-Electricity Data. U.S. Energy Information Administration. URL https://www.eia.gov/electricity/monthly/epm_table_grapher.php?t=epmt_5_3.

EIA-Natural Gas, U.S. Energy Information Administration (EIA) , URL https://www.eia.gov/outlooks/steo/report/natgas.php.

Frischknecht, R., Jungbluth, N., Althaus, H. J., Doka, G., Dones, R., Heck, T., Hellweg, S., Hischier, R., Nemecek, T., Rebitzer, G., Spielmann, M., 2005. The ecoinvent Database: Overview and Methodological Framework (7 pp). Int. J. Life Cycle Assess. 10, 3–9.

Giarola, S., Romain, C., Williams, C.K., Hallett, J.P., Shah, N., 2016. Techno-economic assessment of the production of phthalic anhydride from corn stover. Chem. Eng. Res. Des. 107, 181–194. https://doi.org/https://doi.org/10.1016/j.cherd.2015.10.034

Giarola, S., Shah, N., Bezzo, F., 2012. A comprehensive approach to the design of ethanol supply chains including carbon trading effects. Bioresour. Technol. 107, 175–185. https://doi.org/https://doi.org/10.1016/j.biortech.2011.11.090

Humbird, D., Davis, R.E., Tao, L., Kinchin, C.M., Hsu, D.D., Aden, A., Schoen, P., Lukas, J., Olthof, B., Worley, M., Sexton, D., Dudgeon, D., 2011. Process Design and Economics for Biochemical Conversion of Lignocellulosic Biomass to Ethanol. National Renewable Energy Laboratory, Technical Report NREL/TP-5100-47764.

ICIS, 2017. Indicative Chemical Prices A-Z. URL https://www.icis.com/chemicals/channel-info-chemicals-a-z/.

JBEI, 2009. Joint BioEnergy Institute, URL https://econ.jbei.org/index.php/Materials_and_labor.

Joback, K.G., Reid, R.C., 1987. Estimation of pure-component properties from group-contributions. Chem. Eng. Commun. 57, 233–243. https://doi.org/10.1080/00986448708960487

Jungbluth, N., Chudacoff, M., Dauriat, A., Dinkel, F., Doka, G., Faist Emmenegger, M., Gnansounou, E., Kljun, N., Schleiss, K., Spielmann, M., Stettler, C., Sutter, J., 2007. Ecoinvent v3.4. Life Cycle Inventories of Bioenergy. ecoinvent report No. 17. Dübendorf, CH.

Millar, G.J., Couperthwaite, S.J., Leung, C.W., 2015. An examination of isotherm generation: Impact of bottle-point method upon potassium ion exchange with strong acid cation resin. Sep. Purif. Technol. 141, 366–377. https://doi.org/https://doi.org/10.1016/j.seppur.2014.12.024

Platinum on carbon, 5 wt. % loading, matrix activated carbon support . SIGMA ALDRICH. URL https://www.sigmaaldrich.com/catalog/product/aldrich/205931?lang=en&region=GB (accessed 8.23.18).

Slade, R., Bauen, A., Shah, N., 2009. The greenhouse gas emissions performance of cellulosic ethanol supply chains in Europe. Biotechnol. Biofuels 2, 15. https://doi.org/10.1186/1754-6834-2-15

US EPA, 2009. Technical support document for the nitric acid production sector: Proposed rule for mandatory reporting of greenhouse gases 1–24.

Vasiliu, M., Guynn, K., Dixon, D.A., 2011. Prediction of the Thermodynamic Properties of Key Products and Intermediates from Biomass. J. Phys. Chem. C 115, 15686–15702. https://doi.org/10.1021/jp204243m